

# Dalton Transactions

Accepted Manuscript



This is an *Accepted Manuscript*, which has been through the Royal Society of Chemistry peer review process and has been accepted for publication.

*Accepted Manuscripts* are published online shortly after acceptance, before technical editing, formatting and proof reading. Using this free service, authors can make their results available to the community, in citable form, before we publish the edited article. We will replace this *Accepted Manuscript* with the edited and formatted *Advance Article* as soon as it is available.

You can find more information about *Accepted Manuscripts* in the [Information for Authors](#).

Please note that technical editing may introduce minor changes to the text and/or graphics, which may alter content. The journal's standard [Terms & Conditions](#) and the [Ethical guidelines](#) still apply. In no event shall the Royal Society of Chemistry be held responsible for any errors or omissions in this *Accepted Manuscript* or any consequences arising from the use of any information it contains.

# Group 13 Complexes of Dipyridylmethane, a Forgotten Ligand in Coordination Chemistry

*Petra Vasko,<sup>a</sup> Virva Kinnunen,<sup>a</sup> Jani Moilanen,<sup>a</sup> Tracey L. Roemmele,<sup>b</sup> René T. Boéré,<sup>b</sup> Jari Konu,<sup>a</sup> and Heikki M. Tuononen<sup>\*,a</sup>*

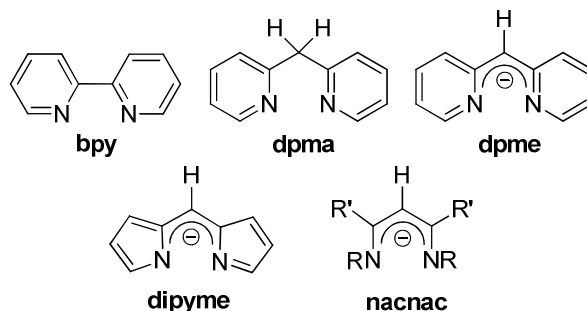
## Abstract

The reactions of dipyridylmethane (dpma) with group 13 trichlorides were investigated in 1:1 and 1:2 molar ratios using NMR spectroscopy and X-ray crystallography. With 1:1 stoichiometry and Et<sub>2</sub>O as solvent, reactions employing AlCl<sub>3</sub> or GaCl<sub>3</sub> gave mixtures of products with the salt [(dpma)<sub>2</sub>MCl<sub>2</sub>]<sup>+</sup>[MCl<sub>4</sub>]<sup>-</sup> (M = Al, Ga) as the main species. The corresponding reactions in 1:2 molar ratio gave similar mixtures but with [(dpma)MCl<sub>2</sub>]<sup>+</sup>[MCl<sub>4</sub>]<sup>-</sup> as the primary product. Pure salts [(dpma)AlCl<sub>2</sub>]<sup>+</sup>[Cl]<sup>-</sup> and [(dpma)AlCl<sub>2</sub>]<sup>+</sup>[AlCl<sub>4</sub>]<sup>-</sup> could be obtained by performing the reactions in CH<sub>3</sub>CN. In the case of InCl<sub>3</sub>, a neutral monoadduct (dpma)InCl<sub>3</sub> formed regardless of the stoichiometry employed. A neutral adduct (dpma)(BCl<sub>3</sub>)<sub>2</sub> was obtained from the reaction between dpma and BCl<sub>3</sub> in Et<sub>2</sub>O using 1:2 stoichiometry. With 1:1 molar ratio of reagents, a mixture of products and deprotonation of the methylene bridge in [(dpma)BCl<sub>2</sub>]<sup>+</sup> was observed. The experimental data showed that the structural flexibility of the dpma ligand results in more diverse coordination chemistry with group 13 elements than that observed for bipyridine (bpy), while computational investigations indicated that the investigated metal-ligand interactions are, to a first approximation, independent of the ligand type. Electrochemical and chemical attempts to reduce the cations [(dpma)MCl<sub>2</sub>]<sup>+</sup> showed that, in stark contrast to the chemistry of the related

$[(\text{bpy})\text{BCl}_2]^+$  cation, the neutral radicals  $[(\text{dpma})\text{MCl}_2]^\bullet$  are extremely unstable. Differences in the redox behaviour of dpma and bpy could be rationalized with the electronic structure of the ligand and that of the methylene bridge in particular. As a whole, the facile reactivity of the methylene bridge in the dpma ligand renders it amenable to further reactivity and functionalization that is not possible in the case of bpy.

## Introduction

The heterocyclic 2,2'-bipyridine (bpy) ligand is one of the cornerstones of modern coordination chemistry. Its ubiquitous nature is best exemplified by the more than 8000 hits found in the Cambridge Crystallographic Database that contain this ligand coordinated to a metal centre.<sup>1</sup> Consequently, the understanding and appreciation of the electronic structure of bpy have shaped the development of many different fields of chemistry. One particularly noteworthy example is metal complexes of bpy with the general formula  $[M(\text{bpy})_3]^{n+}$  and the dication  $[\text{Ru}(\text{bpy})_3]^{2+}$  in particular.<sup>2</sup> The latter is a well-known luminophore<sup>3</sup> whose optical and physicochemical properties make it ideally suited for photochemical applications with recent high-impact examples from bioanalysis<sup>4</sup> and photocatalysis.<sup>5</sup>

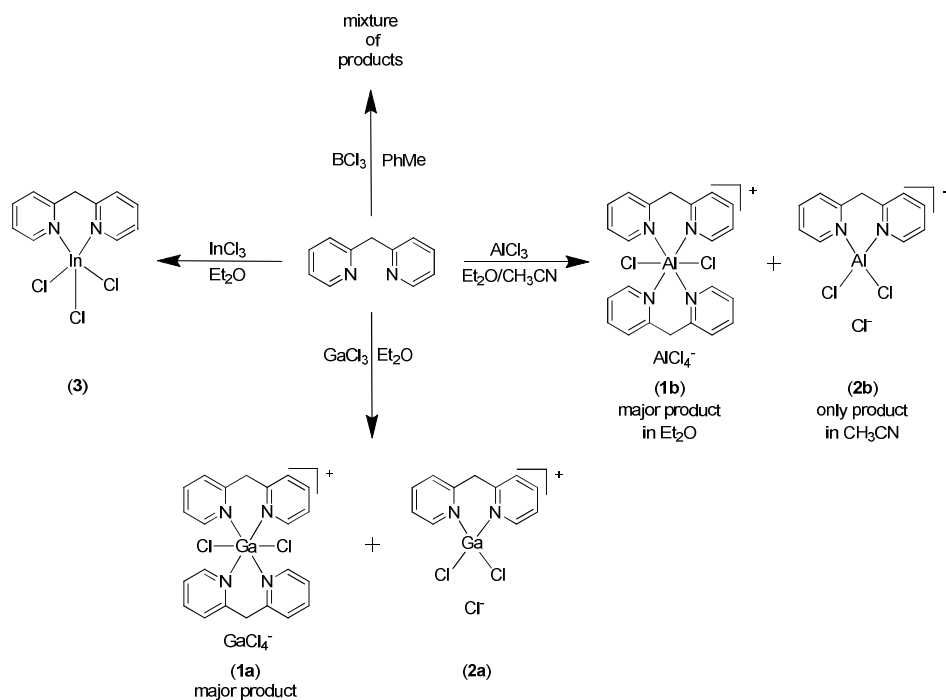
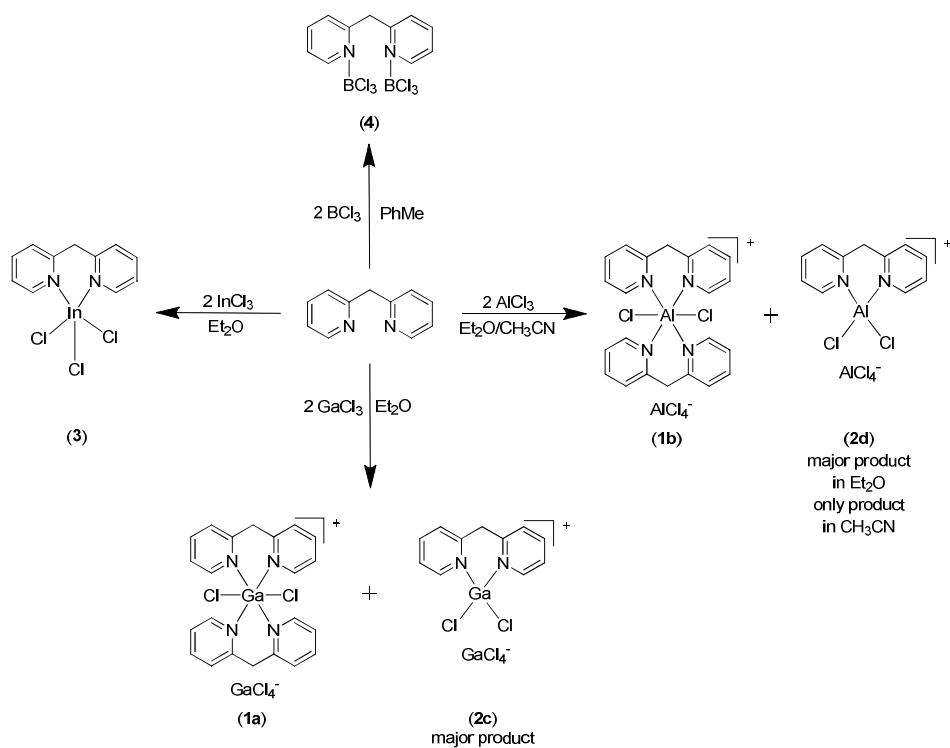


In contrast to the widespread use of bpy as a bidentate chelating ligand, the coordination chemistry of 2,2'-dipyridylmethane (dpma) appears to be significantly underdeveloped with only a handful of extant structurally characterized examples.<sup>1</sup> This is understandable in part as the methylene bridge disrupts the  $\pi$ -conjugation between the pyridyl rings, thereby influencing the photochemical properties of the ligand. Nevertheless, the coordination properties of the dpma ligand have received some attention, particularly in platinum(II) chemistry. Specifically, platinum complexes supported by dpma ligands have recently been shown to activate C–H bonds

in arenes,<sup>6</sup> to undergo oxidative addition with  $\text{CHCl}_3$  and  $\text{CH}_2\text{Cl}_2$ ,<sup>7</sup> and to function as highly efficient catalysts for olefin hydroarylation.<sup>8</sup>

Recently we reported the synthesis of an aluminium complex  $[(\text{dpme})_2\text{Al}]^+$  and its one-electron reduction to the corresponding radical,  $[(\text{dpme})_2\text{Al}]^\bullet$ ,<sup>9</sup> thereby demonstrating the non-innocent behaviour of anionic, deprotonated, 2,2'-dipyridylmethene (dpme) ligand which is analogous to the ubiquitous  $\beta$ -diketiminato (nacnac) framework. This research was motivated by the realization that the structurally related 2,2'-dipyrrromethenes (dipyme) are examples of non-innocent ligands with highly interesting redox properties.<sup>10</sup> As essential background to further studies of the deprotonated dpme ligand, it was necessary to gain a more complete understanding of the coordination chemistry of its neutral precursor, the dpma ligand, with group 13 elements.

Herein we report the results of our investigations on the reactions of dpma with group 13 trichlorides. We describe the synthesis and characterization of ionic aluminium and gallium compounds  $[(\text{dpma})_2\text{MCl}_2]^+[\text{MCl}_4]^-$  (M = Ga (**1a**), Al (**1b**)),  $[(\text{dpma})\text{MCl}_2]^+[\text{Cl}]^-$  (M = Ga (**2a**), Al (**2b**)) and  $[(\text{dpma})\text{MCl}_2]^+[\text{MCl}_4]^-$  (M = Ga (**2c**), Al (**2d**)), as well as that of the neutral indium and boron adducts  $(\text{dpma})\text{InCl}_3 \cdot \text{THF}$  (**3**·THF) and  $(\text{dpma})(\text{BCl}_3)_2$  (**4**). The molecular and electronic structures of **1–4** were examined via combination of crystallographic and computational methods, while their solution behaviour was assessed with NMR spectroscopy. Furthermore, the redox properties of the cations  $[(\text{dpma})\text{MCl}_2]^+$  (M = Al, Ga) were examined using electrochemical techniques. A summary of these reactions and their outcomes is provided in Schemes 1 and 2. Throughout this report, the results will be compared and contrasted with the coordination chemistry of the bpy ligand.

**Scheme 1** Summary of products from 1:1 reactions of dpma with group 13 trichlorides.**Scheme 2** Summary of products from 1:2 reactions of dpma with group 13 trichlorides.

## Experimental section

**Materials and methods.** All reactions and manipulations were performed under an argon atmosphere by using standard Schlenk techniques or an inert atmosphere glovebox. Compounds  $\text{BCl}_3$  (Aldrich, 1.0 M in heptane and 1.0 M in hexanes),  $\text{GaCl}_3$  (Strem, 99.99%),  $\text{InCl}_3$  (Strem, 99.999%), 2-picoline (Aldrich, 98%), 2-fluoropyridine (Aldrich, 98%), *n*-BuLi (Aldrich, 2.5 M in hexanes) and  $[(n\text{-Bu})_4\text{N}]^+[\text{PF}_6]^-$  (Aldrich,  $\geq 99.0\%$ ) were used as received.  $\text{AlCl}_3$  (Riedel-de Haën,  $>98\%$ ) was sublimed prior to use. The solvents were dried and deoxygenated by distillation under an argon atmosphere from appropriate drying agent (Na/benzophenone for *n*-hexane, toluene, THF and  $\text{Et}_2\text{O}$ ;  $\text{CaH}_2$  for  $\text{CH}_2\text{Cl}_2$  and  $\text{CH}_3\text{CN}$ ) and stored over 3–4 Å molecular sieves.

The solvents used for  $^1\text{H}$  and  $^{13}\text{C}\{^1\text{H}\}$  NMR measurements were  $\text{CD}_2\text{Cl}_2$ ,  $\text{CD}_3\text{CN}$ ,  $d_8$ -toluene and  $d_8$ -THF. The room temperature ( $+23\text{ }^\circ\text{C}$ )  $^1\text{H}$  and  $^{13}\text{C}\{^1\text{H}\}$ , as well as variable temperature  $^1\text{H}$  NMR spectra were obtained on a Bruker Avance DPX 250 spectrometer operating at 250.13 MHz, Bruker Avance 300 spectrometer operating at 300.13 MHz, Bruker Avance 400 spectrometer operating at 400.13 MHz, or Bruker Avance DRX 500 spectrometer operating at 500.13 ( $^{13}\text{C}\{^1\text{H}\}$ ) and 125.77 MHz ( $^1\text{H}$ ). All  $^1\text{H}$  and  $^{13}\text{C}\{^1\text{H}\}$  NMR spectra are referenced to the solvent and the chemical shifts are reported relative to  $(\text{CH}_3)_4\text{Si}$ .

Elemental analyses were performed by using a Vario EL *III* Element Analyzer by Elementar Analysensysteme GmbH. Samples for melting point determinations were placed in glass capillaries and sealed with vacuum grease. The temperatures were measured with a Melting Point Apparatus SMP3.

**Crystal structure determinations.** Single crystals of  $[\{(2\text{-NC}_5\text{H}_4)_2\text{CH}_2\}_2\text{GaCl}_2]^+[\text{GaCl}_4]^- \cdot (\text{CH}_2\text{Cl}_2)$  (**1a**· $\text{CH}_2\text{Cl}_2$ ),  $[\{(2\text{-NC}_5\text{H}_4)_2\text{CH}_2\}_2\text{AlCl}_2]^+[\text{AlCl}_4]^- \cdot (\text{C}_4\text{H}_8\text{O})$  (**1b**·THF),  $[\{(2-$

$\text{NC}_5\text{H}_4)_2\text{CH}_2\}\text{GaCl}_2\}^+[\text{GaCl}_4]^-$  (**2c**),  $[\{(2\text{-NC}_5\text{H}_4)_2\text{CH}_2\}\text{InCl}_3]\cdot(\text{C}_4\text{H}_8\text{O})$  (**3**·THF) and  $\{(2\text{-NC}_5\text{H}_4)_2\text{CH}_2\}(\text{BCl}_3)_2$  (**4**) were coated with Fomblin<sup>®</sup> Y oil and mounted on a glass fiber or a MiTeGen loop. Diffraction data were collected on a Bruker-Nonius Kappa Apex II CCD area-detector diffractometer (compounds **1a**, **2c** and **3**) using graphite monochromatized MoK $\alpha$  radiation ( $\lambda = 0.71073 \text{ \AA}$ ) at  $-150 \text{ }^\circ\text{C}$  and on an Agilent SuperNova Dual Source diffractometer equipped with an Atlas CCD area-detector (compounds **1b** and **4**) using graphite monochromatized CuK $\alpha$  radiation ( $\lambda = 1.54184 \text{ \AA}$ ) at  $-150 \text{ }^\circ\text{C}$ . For compounds **1a**, **2c** and **3**, the data were processed using DENZO-SMN v0.93.0 by applying empirical absorption correction, whereas for compounds **1b** and **4**, the data were processed using CrysAlisPro v1.171.36.28 by performing an analytical numeric absorption correction using a multifaceted crystal (as implemented in CrysAlisPro). All structures were solved by direct methods with the help of the SIR-97 program<sup>11</sup> and refined using SHELXL-97<sup>12</sup> within Olex2.<sup>13</sup> After the full-matrix least-squares refinement of all non-hydrogen atoms with anisotropic thermal parameters, the hydrogen atoms were placed in calculated (idealized) positions. The isotropic thermal parameters of the hydrogen atoms were fixed at 1.2 times that of the respective heavy atoms and they were treated as riding atoms in the final refinement. For details of the crystallographic data, see ESI<sup>†</sup>.

**Electrochemical experiments.** Cyclic voltammetry experiments were carried out using a Princeton Applied Research PARSTAT 2273 potentiostat. A conventional three electrode cell fitted with a platinum or glassy carbon working electrode, a platinum counter electrode and a silver reference electrode was used in all measurements. The cyclic voltammograms (CVs) were recorded at  $+21 \pm 2 \text{ }^\circ\text{C}$  using solutions  $\sim 5 \text{ mM}$  in analyte in freshly distilled  $\text{CH}_3\text{CN}$  or  $\text{CH}_2\text{Cl}_2$  which were  $0.4 \text{ M}$  in  $[(n\text{-Bu})_4\text{N}]^+[\text{PF}_6]^-$  supporting electrolyte. All CVs were referenced against an internal standard ( $\sim 5 \text{ mM}$  ferrocene) and measured using scan rates between  $0.1$  and  $10 \text{ Vs}^{-1}$ .

**Computational details.** All calculations were done with the Gaussian 09 program package.<sup>14</sup> The geometries of studied systems were optimized in the gas phase with density functional theory (DFT) using the hybrid PBE1PBE exchange-correlation functional<sup>15</sup> in combination with the def-TZVP basis sets.<sup>16</sup> Frequency calculations were performed for all stationary points found to find out their nature on the potential energy hypersurface.

**Synthesis of (2-NC<sub>5</sub>H<sub>4</sub>)<sub>2</sub>CH<sub>2</sub> (dpma).** The neutral ligand (2-NC<sub>5</sub>H<sub>4</sub>)<sub>2</sub>CH<sub>2</sub> (dpma) was prepared according to a literature procedure giving a yellow oily product in 51% yield.<sup>17</sup> <sup>1</sup>H NMR (*d*<sub>8</sub>-THF, +23 °C): δ 4.25 [s, 2H, (2-NC<sub>5</sub>H<sub>4</sub>)<sub>2</sub>CH<sub>2</sub>], 7.08–8.45 [8H, (2-NC<sub>5</sub>H<sub>4</sub>)<sub>2</sub>CH<sub>2</sub>], <sup>1</sup>H NMR (CD<sub>3</sub>CN, +23 °C): δ 4.25 [s, 2H, (2-NC<sub>5</sub>H<sub>4</sub>)<sub>2</sub>CH<sub>2</sub>], 7.15–8.46 [8H, (2-NC<sub>5</sub>H<sub>4</sub>)<sub>2</sub>CH<sub>2</sub>].

**Synthesis of [(dpma)<sub>2</sub>GaCl<sub>2</sub>]<sup>+</sup>[GaCl<sub>4</sub>]<sup>-</sup> (1a).** A solution of dpma (0.170 g, 1.00 mmol) in 10 mL of Et<sub>2</sub>O was cooled to -78 °C and a solution of GaCl<sub>3</sub> (0.176 g, 1.00 mmol) in 10 mL of Et<sub>2</sub>O was added via cannula. The reaction mixture was stirred for 10 min at -78 °C and 2 h at room temperature, after which the precipitate was allowed to settle and the solvent was decanted via cannula. The product was washed with Et<sub>2</sub>O (1 × 5 mL) and dried under vacuum, giving **1a** as a white powder (0.350 g, 95% calculated as **1a**). Crystals suitable for single crystal X-ray diffraction measurement were grown by slow diffusion from CH<sub>2</sub>Cl<sub>2</sub> and *n*-hexane. Melting point: 91–92 °C (sample turns to yellow before melting). <sup>1</sup>H NMR (*d*<sub>8</sub>-THF, +23 °C): δ 4.14 [br, 4H, (2-NC<sub>5</sub>H<sub>4</sub>)<sub>2</sub>CH<sub>2</sub>], 7.58–8.99 [16H, (2-NC<sub>5</sub>H<sub>4</sub>)<sub>2</sub>CH<sub>2</sub>]; (*d*<sub>8</sub>-THF, -80 °C): δ 3.34 [d, 1H, (2-NC<sub>5</sub>H<sub>4</sub>)<sub>2</sub>CH<sub>2</sub>], 4.40 [d, 1H, (2-NC<sub>5</sub>H<sub>4</sub>)<sub>2</sub>CH<sub>2</sub>], 4.62 [s, 2H, (2-NC<sub>5</sub>H<sub>4</sub>)<sub>2</sub>CH<sub>2</sub>], 7.52–9.90 [24H, (2-NC<sub>5</sub>H<sub>4</sub>)<sub>2</sub>CH<sub>2</sub>]. <sup>13</sup>C{<sup>1</sup>H} NMR (*d*<sub>8</sub>-THF, +23 °C): δ 40.9 [(2-NC<sub>5</sub>H<sub>4</sub>)<sub>2</sub>CH<sub>2</sub>], 125.1–156.1 [(2-NC<sub>5</sub>H<sub>4</sub>)<sub>2</sub>CH<sub>2</sub>]. Anal. Calcd. for C<sub>22</sub>H<sub>20</sub>Ga<sub>2</sub>Cl<sub>6</sub>N<sub>4</sub>: C, 38.15; N, 8.09; H, 2.91. Found: C, 37.62; N, 7.89; H, 3.32.

**Synthesis of [(dpma)AlCl<sub>2</sub>]<sup>+</sup>[Cl]<sup>-</sup> (2b).** A solution of dpma (0.170 g, 1.00 mmol) in 15 mL of CH<sub>3</sub>CN was cooled to -50 °C and a solution of AlCl<sub>3</sub> (0.133 g, 1.00 mmol) in 15 mL of CH<sub>3</sub>CN was added via cannula. The reaction mixture was first stirred for 15 min at -50 °C and then *ca.* 16 h at +55 °C. The solvent was evaporated and the precipitate was washed with Et<sub>2</sub>O (2 × 5 mL) and dried under vacuum, which gave **2b** as a pale yellow powder (0.200 g, 66%). Melting point: 104–105 °C (sample turns to yellow before melting). <sup>1</sup>H NMR (CD<sub>3</sub>CN, +23 °C): δ 4.61 [s, 2H, (2-NC<sub>5</sub>H<sub>4</sub>)<sub>2</sub>CH<sub>2</sub>], 7.55–8.62 [8H, (2-NC<sub>5</sub>H<sub>4</sub>)<sub>2</sub>CH<sub>2</sub>]. <sup>13</sup>C {<sup>1</sup>H} NMR (CD<sub>3</sub>CN, +23 °C): δ 40.3 [(2-NC<sub>5</sub>H<sub>4</sub>)<sub>2</sub>CH<sub>2</sub>], 124.8–156.5 [(2-NC<sub>5</sub>H<sub>4</sub>)<sub>2</sub>CH<sub>2</sub>]. Anal. Calcd. for C<sub>22</sub>H<sub>20</sub>Al<sub>2</sub>Cl<sub>6</sub>N<sub>4</sub>: C, 43.52; N, 9.23; H, 3.32. Found: C, 42.63; N, 9.29; H, 3.57.

**Reaction between dpma and AlCl<sub>3</sub> in Et<sub>2</sub>O in 1:1 molar ratio.** A solution of dpma (0.170 g, 1.00 mmol) in 10 mL of Et<sub>2</sub>O was cooled to -78 °C and a solution of AlCl<sub>3</sub> (0.133 g, 1.00 mmol) in 10 mL of Et<sub>2</sub>O was added via cannula. The reaction mixture was stirred for 15 min at -78 °C and 1.5 h at room temperature, after which the precipitate was allowed to settle and the solvent was decanted via cannula. The product was washed with Et<sub>2</sub>O (1 × 5 mL) and dried under vacuum, giving a white powder (0.263 g). Characterization of the powder via <sup>1</sup>H NMR showed it to be a mixture of **1b** and **2b**; for further details, see main text and ESI†. Crystals of **1b**, [(dpma)<sub>2</sub>AlCl<sub>2</sub>]<sup>+</sup>[AlCl<sub>4</sub>]<sup>-</sup>, suitable for single crystal X-ray diffraction measurement were grown by slow diffusion from THF and *n*-hexane.

**Synthesis of [(dpma)GaCl<sub>2</sub>]<sup>+</sup>[GaCl<sub>4</sub>]<sup>-</sup> (2c).** A solution of dpma (0.170 g, 1.00 mmol) in 10 mL of Et<sub>2</sub>O was cooled to -78 °C and a solution of GaCl<sub>3</sub> (0.350 g, 2.00 mmol) in 10 mL of Et<sub>2</sub>O was added via cannula. The reaction mixture was stirred for 10 min at -78 °C and 2 h at room temperature, after which the precipitate was allowed to settle and the solvent was decanted via cannula. The product was washed with 5 mL of Et<sub>2</sub>O and dried under vacuum, giving **2c** as a

white powder (0.500 g, 88% calculated as **2c**). Crystals suitable for single crystal X-ray diffraction measurement were grown slowly from a saturated solution of toluene. Melting point: 151–153 °C (sample turns to yellow before melting).  $^1\text{H}$  NMR ( $d_8$ -THF, +23 °C):  $\delta$  4.75 [br, 2H, (2-NC<sub>5</sub>H<sub>4</sub>)<sub>2</sub>CH<sub>2</sub>], 7.81–8.97 [8H, (2-NC<sub>5</sub>H<sub>4</sub>)<sub>2</sub>CH<sub>2</sub>]. ]; ( $d_8$ -THF, –60 °C):  $\delta$  3.34 [d, 1H, (2-NC<sub>5</sub>H<sub>4</sub>)<sub>2</sub>CH<sub>2</sub>], 4.40 [d, 1H, (2-NC<sub>5</sub>H<sub>4</sub>)<sub>2</sub>CH<sub>2</sub>], 4.97 [s, 2H, (2-NC<sub>5</sub>H<sub>4</sub>)<sub>2</sub>CH<sub>2</sub>], 7.91–9.00 [8H, (2-NC<sub>5</sub>H<sub>4</sub>)<sub>2</sub>CH<sub>2</sub>], 7.55–9.88 [16H, (2-NC<sub>5</sub>H<sub>4</sub>)<sub>2</sub>CH<sub>2</sub>].  $^{13}\text{C}\{^1\text{H}\}$  NMR ( $d_8$ -THF, +23 °C):  $\delta$  40.1 [(2-NC<sub>5</sub>H<sub>4</sub>)<sub>2</sub>CH<sub>2</sub>], 126.4–155.6 [(2-NC<sub>5</sub>H<sub>4</sub>)<sub>2</sub>CH<sub>2</sub>]. Anal. Calcd. for C<sub>11</sub>H<sub>10</sub>Ga<sub>2</sub>Cl<sub>6</sub>N<sub>2</sub>: C, 25.29; N, 5.36; H, 1.93. Found: C, 25.65; N, 5.39; H, 2.39.

**Synthesis of [(dpma)AlCl<sub>2</sub>]<sup>+</sup>[AlCl<sub>4</sub>]<sup>–</sup> (**2d**).** A solution of dpma (0.170 g, 1.00 mmol) in 10 mL of CH<sub>3</sub>CN was cooled to –50 °C and a solution of AlCl<sub>3</sub> (0.266 g, 2.00 mmol) in 10 mL of CH<sub>3</sub>CN was added via cannula. The reaction mixture was first stirred for 5 min at –50 °C and then *ca.* 16 h at +55 °C. The solvent was evaporated and the precipitate was washed with Et<sub>2</sub>O (3 × 5 mL) and dried under vacuum, giving **2d** as a pale yellow powder (0.360 g, 82%). Melting point: 217–218 °C (sample turns to yellow before melting).  $^1\text{H}$  NMR (CD<sub>3</sub>CN, +23 °C):  $\delta$  5.00 [s, 2H, (2-NC<sub>5</sub>H<sub>4</sub>)<sub>2</sub>CH<sub>2</sub>], 7.92–8.69 [8H, (2-NC<sub>5</sub>H<sub>4</sub>)<sub>2</sub>CH<sub>2</sub>].  $^{13}\text{C}\{^1\text{H}\}$  NMR (CD<sub>3</sub>CN, +23 °C):  $\delta$  36.5 [(2-NC<sub>5</sub>H<sub>4</sub>)<sub>2</sub>CH<sub>2</sub>], 127.1–152.0 [(2-NC<sub>5</sub>H<sub>4</sub>)<sub>2</sub>CH<sub>2</sub>]. Anal. Calcd. for C<sub>11</sub>H<sub>10</sub>Al<sub>2</sub>Cl<sub>6</sub>N<sub>2</sub>: C, 30.24; N, 6.41; H, 2.31. Found: C, 30.59; N, 6.97; H, 2.49.

**Reaction between dpma and AlCl<sub>3</sub> in Et<sub>2</sub>O in 1:2 molar ratio.** A solution of dpma (0.170g, 1.00 mmol) in 10 mL of Et<sub>2</sub>O was cooled to –78 °C and a solution of AlCl<sub>3</sub> (0.267 g, 2.00 mmol) in 10 mL of Et<sub>2</sub>O was added via cannula. The reaction mixture was stirred for 10 min at –78 °C and 1.5 h at room temperature, after which the precipitate was allowed to settle and the solvent was decanted via cannula. The product was washed with Et<sub>2</sub>O (1 × 5 mL) and dried under vacuum, giving a white powder (0.307 g). Characterization of the product via  $^1\text{H}$  NMR showed it

to be a mixture of **1b** and **2d**; for further details, see main text and ESI†. Crystals of **1b**,  $[(\text{dpma})_2\text{AlCl}_2]^+[\text{AlCl}_4]^-$ , suitable for single crystal X-ray diffraction measurement were grown by slow diffusion from THF and *n*-hexane.

**Synthesis of (dpma)InCl<sub>3</sub> (3).** A solution of dpma (0.170 g, 1.00 mmol) in 10 mL of Et<sub>2</sub>O was cooled to  $-78$  °C and a solution of InCl<sub>3</sub> (0.221 g, 1.00 mmol) in 10 mL of Et<sub>2</sub>O was added via cannula. The reaction mixture was stirred for 10 min at  $-78$  °C and 3 h at room temperature, after which the precipitate was allowed to settle and the solvent was decanted. The product was dried under vacuum, giving **3** as a pale yellow powder (0.360 g, 92%). The same synthesis was also performed using 1:2 ratio between dpma (0.170 g, 1.00 mmol) and InCl<sub>3</sub> (0.442 g, 2.00 mmol), yielding a pale yellow powder (0.532 g) that was spectroscopically and crystallographically identical to **3**. Crystals suitable for single crystal X-ray diffraction measurement were obtained by slow diffusion from THF and *n*-hexane. Melting point: 226–229 °C. <sup>1</sup>H NMR (*d*<sub>8</sub>-THF, +23 °C):  $\delta$  5.09 [s, 2H, (2-NC<sub>5</sub>H<sub>4</sub>)<sub>2</sub>CH<sub>2</sub>], 7.58–9.17 [8H, (2-NC<sub>5</sub>H<sub>4</sub>)<sub>2</sub>CH<sub>2</sub>]. <sup>13</sup>C{<sup>1</sup>H} NMR spectrum could not be obtained owing to poor solubility of **3** in common deuterated solvents. Anal. Calcd. for C<sub>11</sub>H<sub>10</sub>Cl<sub>3</sub>InN<sub>2</sub>: C, 33.76; N, 7.16; H, 2.58. Found: C, 34.04; N, 7.05; H, 3.19.

**Synthesis of (dpma)(BCl<sub>3</sub>)<sub>2</sub> (4).** A solution of dpma (0.142 g, 0.82 mmol) in 15 mL of Et<sub>2</sub>O was cooled to  $-78$  °C and a solution of BCl<sub>3</sub> (1.6 mL, 1.60 mmol) in hexanes was added via syringe. The reaction mixture was stirred for 10 min at  $-78$  °C, which resulted in formation of an off-white precipitate. The stirring was continued for one hour at room temperature after which the solvent was decanted and the precipitate was dried under vacuum, giving **4** as an off-white powder (0.289 g, 86%). Crystals suitable for single crystal X-ray diffraction measurement were obtained by slow diffusion from CH<sub>2</sub>Cl<sub>2</sub> and *n*-hexane. Melting point: 138–141 °C (sample turns to red before melting). <sup>1</sup>H NMR (CD<sub>2</sub>Cl<sub>2</sub>, +23 °C):  $\delta$  6.25 [s, 2H, (2-NC<sub>5</sub>H<sub>4</sub>)<sub>2</sub>CH<sub>2</sub>], 7.43–9.82

[8H, (2-NC<sub>5</sub>H<sub>4</sub>)<sub>2</sub>CH<sub>2</sub>]. <sup>13</sup>C{<sup>1</sup>H} NMR (CD<sub>2</sub>Cl<sub>2</sub>, +23 °C): δ 41.9 ((2-NC<sub>5</sub>H<sub>4</sub>)<sub>2</sub>CH<sub>2</sub>), 124.6–157.7 [(2-NC<sub>5</sub>H<sub>4</sub>)<sub>2</sub>CH<sub>2</sub>]. Anal. Calcd. for C<sub>11</sub>H<sub>10</sub>B<sub>2</sub>Cl<sub>6</sub>N<sub>2</sub>: C, 32.66; N, 6.92; H, 2.49. Found: C, 33.65; N, 6.92; H, 3.18.

**Reaction between dpma and BCl<sub>3</sub> in toluene in 1:1 molar ratio.** A solution of BCl<sub>3</sub> in hexanes (1.0 mL, 1.00 mmol) was added to a stirred solution of dpma (0.170 g, 1.00 mmol) in toluene at –78 °C. After stirring for 3 h at room temperature, a yellow-orange precipitate was formed. The precipitate was allowed to settle, after which the red solution was decanted and both phases dried under vacuum. Subsequent <sup>1</sup>H NMR studies showed that the solvent phase contains a mixture of products, whereas the precipitate was found to be the salt [H<sub>2</sub>(dpma)]<sup>2+</sup>[Cl]<sup>–</sup>[BCl<sub>4</sub>]<sup>–</sup>, as confirmed by recrystallization via slow diffusion from CH<sub>2</sub>Cl<sub>2</sub> and pentane; for further details, see main text and ESI†.

The equimolar reaction between dpma and BCl<sub>3</sub> was also done by adding a combined solution of triethylamine (0.109 g, 1.08 mmol) and BCl<sub>3</sub> in hexanes (1.0 mL, 1.00 mmol) to a stirred solution of dpma (0.173 mg, 1.00 mmol) in toluene at –78 °C. Stirring of the reaction mixture at +45°C for 8 h gave a red solution and a light orange precipitate. Subsequent <sup>1</sup>H NMR studies showed the light orange precipitate to be the salt [Et<sub>3</sub>NH]<sup>+</sup>[Cl]<sup>–</sup>, whereas the red solution was found to contain the complex (dpme)BCl<sub>2</sub>; for further details, see main text and ESI†.

## Results and discussion

### Reactions of dipyridylmethane (dpma) with $MCl_3$ ( $M = Al, Ga$ ) in 1:1 molar ratio. A

reaction between dpma and  $GaCl_3$  was carried out in 1:1 molar ratio at  $-78\text{ }^\circ\text{C}$  in  $Et_2O$ . A white precipitate formed immediately and after an appropriate reaction time, the product was separated from the solution, washed and dried to afford a white powder in excellent yield (95 %).

Compound **1a** was crystallized as colourless single crystals suitable for X-ray diffraction studies from a 1:1 mixture of  $CH_3CN$  and *n*-hexane (Fig. 1). The solid state structure of **1a** shows that it consists of discrete tetrahedral  $[GaCl_4]^-$  anions and octahedral  $[cis-(dpma)_2GaCl_2]^+$  cations packed in alternating layers with no significant close contacts between the two; molecules of crystallization solvent ( $CH_2Cl_2$ ) fill the remaining cavities in the lattice. The structure of the cation has  $C_2$  symmetry and adopts a *cis*-conformation. The key bond parameters of the cation in **1a** show two nearly identical and distinctively bent dpma ligands, each with a bridge N-C-C-C dihedral angle close to  $60^\circ$ ; the bending of the ligand framework in **1a** is similar to other known main group metal complexes incorporating the dpma ligand.<sup>18</sup> The crystal structure of **1a** shows the methylene hydrogens to be inequivalent and remote from the two chlorine atoms. The average Ga-N bond length in **1a** is 2.125(4) Å which is slightly longer than that in an analogous salt containing the bpy ligand,  $[(bpy)_2GaCl_2]^+[GaCl_4]^-$ , 2.103(2) Å; the Ga-Cl distances are also comparable between these structures.<sup>19</sup>

The room temperature  $^1H$  NMR spectrum from the product (in  $d_8$ -THF) shows a singlet at 4.14 ppm and four multiplets from 7.58 to 8.99 ppm (see Fig. S1 in ESI†). Although all signals are of equal intensity, as expected, the singlet corresponding to the methylene hydrogens is extremely broad, as is also the case for one of the multiplets in the aromatic region. This strongly indicates the presence of a dynamic process in solution. Consequently, the reaction product was further

investigated by variable temperature (VT)  $^1\text{H}$  NMR spectroscopy (see ESI† for details). The VT  $^1\text{H}$  NMR experiments (in  $d_8$ -THF) revealed that there is a second species in solution in addition to **1a** and we assigned it to the salt  $[(\text{dpma})\text{GaCl}_2]^+[\text{Cl}]^-$  (**2a**) based on the equilibrium  $[(\text{dpma})_2\text{GaCl}_2]^+[\text{GaCl}_4]^- \rightleftharpoons 2[(\text{dpma})\text{GaCl}_2]^+[\text{Cl}]^-$ . The relative intensities of the  $^1\text{H}$  NMR signals reveal that the dynamic ligand redistribution process favours **1a** over **2a** in *ca.* 9:1 ratio at  $-80$  °C with the relative concentration of **2a** increasing as the temperature is increased. More detailed NMR investigations revealed that the dynamic process is not only temperature but also solvent dependent. While the room temperature  $^1\text{H}$  NMR spectrum of the product in  $\text{CD}_2\text{Cl}_2$  is similar to that in  $d_8$ -THF (see Fig. S3 in ESI†), a complete conversion to  $[(\text{dpma})\text{GaCl}_2]^+[\text{Cl}]^-$  *i.e.* **2a** takes place rapidly in  $\text{CD}_3\text{CN}$  (see Fig. S4 in ESI†). However, **2a** was found to be unstable in  $\text{CD}_3\text{CN}$  and it decomposes gradually into the free dpma ligand as well as to other uncharacterized products.

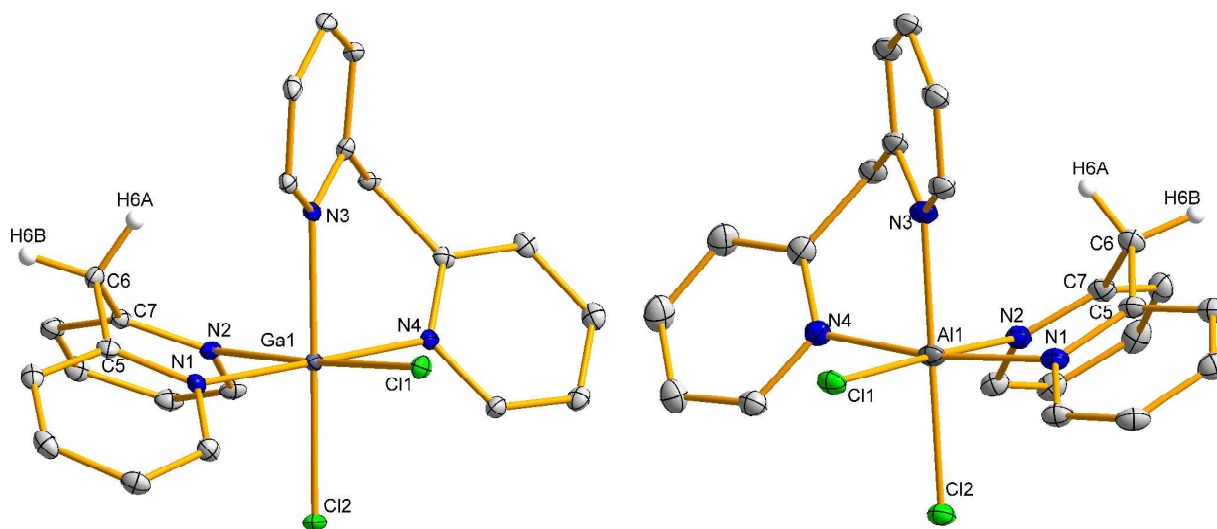


**Fig. 1** Thermal ellipsoid plots (30% probability) of the cations  $[(\text{dpma})_2\text{GaCl}_2]^+$  (left) and  $[(\text{dpma})_2\text{AlCl}_2]^+$  (right) as found in the crystal structures of the salts  $[(\text{dpma})_2\text{MCl}_2]^+[\text{MCl}_4]^-$  ( $\text{M} = \text{Ga}$  (**1a**),  $\text{Al}$  (**1b**)). Only C(6) bound hydrogen atoms are shown for clarity.

Having therefore established the salt [*cis*-(dpma)<sub>2</sub>GaCl<sub>2</sub>]<sup>+</sup>[GaCl<sub>4</sub>]<sup>-</sup> (**1a**) as the preferred product from the 1:1 reaction between dpma and GaCl<sub>3</sub> in Et<sub>2</sub>O, we set our target to the synthesis of its aluminium analogue [(dpma)<sub>2</sub>AlCl<sub>2</sub>]<sup>+</sup>[AlCl<sub>4</sub>]<sup>-</sup> (**1b**). Similarly to the synthesis of **1a**, the reaction between dpma and AlCl<sub>3</sub> was carried out in 1:1 molar ratio by the addition of the metal halide at -78 °C in Et<sub>2</sub>O, which resulted in an immediate formation of a white precipitate. After an appropriate reaction time and separation from the mother liquor, a white powdery product was isolated in good yield (87%).

In view of the previously observed solution behaviour of **1a**, the product was first characterized by <sup>1</sup>H NMR spectroscopy (in *d*<sub>8</sub>-THF, see Fig. S5 in ESI†) which in this instance revealed a well-resolved spectrum even at room temperature that clearly shows a mixture of two major products as judged by the number and intensity of signals in the aliphatic region: a singlet at 4.43 ppm as well as two AB doublets at 3.09 and 4.33 ppm (<sup>2</sup>J(<sup>1</sup>H,<sup>1</sup>H) = 17.5 Hz). These spectral features, as well as the pattern of several equal intensity multiplets in the aromatic region, can be compared to the <sup>1</sup>H NMR data for the mixture of **1a** and **2a** (see ESI† for details), which allows the assignment of the main products from the AlCl<sub>3</sub> reaction as [*cis*-(dpma)<sub>2</sub>AlCl<sub>2</sub>]<sup>+</sup>[AlCl<sub>4</sub>]<sup>-</sup> (**1b**) and [(dpma)AlCl<sub>2</sub>]<sup>+</sup>[Cl]<sup>-</sup> (**2b**) in *ca.* 2:1 ratio.

When measuring the <sup>1</sup>H NMR spectra of the **1b:2b** mixture in different solvents, it was found that a complete conversion to **2b** takes place rapidly in CD<sub>3</sub>CN. However, unlike for **1a**, repeated <sup>1</sup>H NMR measurements for **2b** in CD<sub>3</sub>CN showed no change in the spectral data. Consequently, the 1:1 reaction between dpma and AlCl<sub>3</sub> was repeated in CH<sub>3</sub>CN, yielding **2b** as a pure product. The room temperature <sup>1</sup>H NMR spectrum of **2b** (in CD<sub>3</sub>CN) shows a singlet for the bridging methylene hydrogens at 4.61 ppm and four multiplets for the pyridyl hydrogens from 7.55 to 8.62 ppm (see Fig. S6 in ESI†).<sup>20</sup>

Despite extensive crystallization efforts, we were not able to grow single crystals of **2b** from CH<sub>3</sub>CN. However, colourless crystals suitable for single crystal X-ray structural studies were obtained using a mixture of THF and *n*-hexane as the solvent system. A subsequent structure determination showed that the crystals actually contain the salt  $[cis-(dpma)_2AlCl_2]^+[AlCl_4]^-$  *i.e.* **1b** that is analogous to **1a** (Fig. 1). The preferred crystallization of **1b** over **2b** from THF and *n*-hexane solvent system is not overly surprising taking into account that a mixture of products was seen in the <sup>1</sup>H NMR in *d*<sub>8</sub>-THF. The cation in **1b** is close to ideal C<sub>2</sub> symmetry and adopts *cis*-conformation with respect to the two chloride atoms. The key metrical parameters of the dpma ligands in **1b** are virtually identical to that in **1a** (see Table S2 in ESI†) and the M-N and M-Cl bond lengths are only slightly shorter for M = Al, as expected due to the d-block contraction in Ga. We note that the local coordination environment of the metal centre in  $[cis-(dpma)_2AlCl_2]^+$  is very similar to that of the analogous complex with bpy,  $[(bpy)_2AlCl_2]^+[Cl]^-$ ,<sup>21</sup> despite the significant puckering of the coordinated dpma ligand.

**Reactions of dipyridylmethane (dpma) with MCl<sub>3</sub> (M = Al, Ga) in 1:2 molar ratio.** Since the reactions between dpma and MCl<sub>3</sub> turned out to be more complex than anticipated, we were also interested in examining them using a 1:2 molar ratio of the reagents. The synthesis between 1 equivalent of dpma and 2 equivalents of GaCl<sub>3</sub> was carried out by the addition of the metal halide at -78 °C in Et<sub>2</sub>O. A white precipitate formed immediately after the addition of GaCl<sub>3</sub> and the product was isolated as a white powder after workup in good yield (88%).

The room temperature <sup>1</sup>H NMR spectrum (in *d*<sub>8</sub>-THF) recorded for the product is similar to that of **1a** (see Fig. S7 in ESI†): a broad singlet for the methylene hydrogens is observed at 4.75 ppm, whereas the pyridyl bound hydrogens show a set of multiplets between 7.81 and 8.97 ppm.

The broadness of the observed signals suggests that a ligand redistribution process is again occurring, which prompted us to conduct VT  $^1\text{H}$  NMR studies also for this compound (see ESI† for details). As in the case of **1a**, the solution was found to contain two major species in a temperature dependent equilibrium. An analysis of the NMR data allows the identification of the products as the salts  $[(\text{dpma})\text{GaCl}_2]^+[\text{GaCl}_4]^-$  (**2c**) and  $[\text{cis}-(\text{dpma})_2\text{GaCl}_2]^+[\text{GaCl}_4]^-$  (**1a**) in *ca.* 4:1 ratio at  $-60\text{ }^\circ\text{C}$ ; the salt **2c** remains the preferred product also at higher temperatures. Subsequent  $^1\text{H}$  NMR studies in different deuterated solvents showed that the dynamic equilibrium observed for **2c** is solvent dependent. In  $\text{CD}_2\text{Cl}_2$ , the NMR data are consistent with **2c** being the only species present in solution (see Fig. S9 in ESI†), whereas a very small amount of **1a** is visible in  $\text{CD}_3\text{CN}$  with no indication of a dynamic process that is faster than the NMR timescale (see Fig. S10 in ESI†).

The above spectral interpretation is supported by results from crystallization studies that yielded excellent quality colourless single crystals of the salt **2c** (Fig. 2) when using toluene as the crystallization solvent. The solid state structure displays distinct  $[\text{GaCl}_4]^-$  anions and  $[(\text{dpma})\text{GaCl}_2]^+$  cations, the latter having the expected  $C_s$  symmetric structure. The Ga-N bond lengths in the cation are somewhat shorter than those in **1a** (see Table S2 in ESI†), mainly owing to the difference in the metal coordination number. All other bond lengths and angles involving the *N,N'*-chelated ligand are comparable between the two structures, including the bending of the ligand backbone. While there are no reports of structurally characterized complexes of the type  $[(\text{bpy})\text{GaX}_2]^+$  ( $X = \text{halogen}$ ), the metrical parameters of the dpma ligand in **2c** can be compared to those in a related thallium salt,  $[(\text{dpma})\text{TlMe}_2]^+[\text{NO}_3]^-$ ,<sup>18c</sup> which shows major differences only in torsional angles and metal-ligand bond lengths. This can be attributed to different coordination environment at the metal: tetrahedral for  $[(\text{dpma})\text{GaCl}_2]^+$  and disphenoidal for  $[(\text{dpma})\text{TlMe}_2]^+$ .

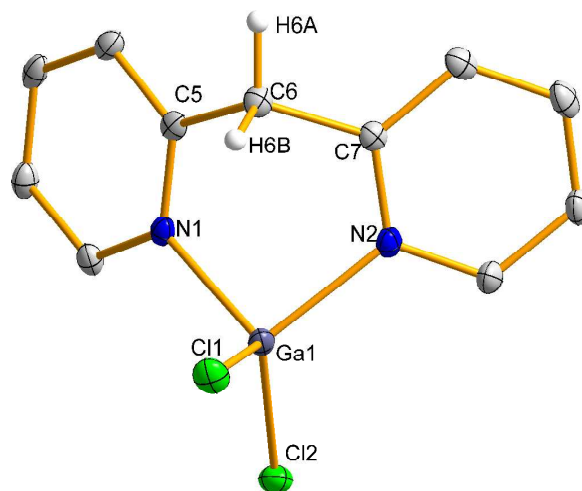


**Fig. 2** Thermal ellipsoid plot (30% probability) of the cation  $[(dpma)GaCl_2]^+$  in the salt  $[(dpma)GaCl_2]^+[GaCl_4]^-$  (**2c**). Hydrogen atoms in the pyridyl rings have been omitted for clarity.

If the reaction between the dpma ligand and  $AlCl_3$  is performed in 1:2 molar ratio in  $Et_2O$ , a product mixture similar to that found in the case of **1b** is seen in the  $^1H$  NMR spectrum (in  $d_8$ -THF, see Fig. S11 in ESI†). Consequently, the reaction was performed in  $CH_3CN$  at  $-50$  °C, giving a pale yellow powder, presumed to be the salt  $[(dpma)AlCl_2]^+[AlCl_4]^-$  (**2d**), after removal of volatiles. The  $^1H$  NMR spectrum of the product (in  $CD_3CN$ ) shows a single species and no signs of ligand redistribution (see Fig. S12 in ESI†).<sup>20</sup> a sharp singlet for the methylene hydrogens is observed at 5.00 ppm, while four multiplets for the pyridyl hydrogens are seen from 7.92 to 8.69 ppm. Hence, the  $^1H$  NMR data for **2d** is nearly identical to that of  $[(dpma)GaCl_2]^+[GaCl_4]^-$ , as should be the case for two structurally similar compounds that differ only in the identity of the group 13 element.

Unfortunately we were not able to grow single crystals of **2d** from  $CH_3CN$ . In addition, crystallization attempts from ethereal solvents again resulted in the characterization of the salt  $[cis-(dpma)_2AlCl_2]^+[AlCl_4]^-$  *i.e.* **1b**. Due to our inability to obtain crystallographic data for both

**2d** and **2b**, we sought a way to ensure that they have been properly identified. Hence, one equivalent of  $\text{AlCl}_3$  (in toluene) was added to a  $\text{CH}_3\text{CN}$  solution of **2b** as this should result in formation of the  $[\text{AlCl}_4]^-$  anion and, hence, the salt **2d**:  $[(\text{dpma})\text{AlCl}_2]^+[\text{Cl}]^-$  (**2b**) +  $\text{AlCl}_3 \rightarrow [(\text{dpma})\text{AlCl}_2]^+[\text{AlCl}_4]^-$  (**2d**). The reaction was performed at  $+55\text{ }^\circ\text{C}$  and monitored by  $^1\text{H}$  NMR spectroscopy (in  $\text{CD}_3\text{CN}$ ). As expected, the addition of  $\text{AlCl}_3$  results in a characteristic downfield shift of the singlet associated to the methylene hydrogens from 4.61 (**2b**) to 5.02 ppm, thereby yielding a  $^1\text{H}$  NMR spectrum that is identical to that of pure **2d** (see Fig. S13 in ESI†). We also note that a similar trend is seen in the  $^1\text{H}$  NMR data of the gallium analogues **2a** and **2c**, in which case the singlet shifts similarly from 4.62 to 4.97 ppm (in  $d_8$ -THF).

**Reactions of dipyridylmethane (dpma) with  $\text{InCl}_3$  in 1:1 and 1:2 molar ratios.** In a similar fashion to the synthesis of **1a**, the reaction between dpma and  $\text{InCl}_3$  was performed in 1:1 stoichiometry at  $-78\text{ }^\circ\text{C}$  in  $\text{Et}_2\text{O}$ . A pale yellow precipitate formed immediately upon addition of  $\text{InCl}_3$ . After stirring for 3 h at room temperature, a yellow powder was isolated in excellent yield (92%). Crystals suitable for a single crystal X-ray structure determination were grown from the powder by slow diffusion of *n*-hexane into a THF solution. All attempts to grow crystals of **3** from non-coordinating solvents failed due to the low solubility of the product.

The room temperature  $^1\text{H}$  NMR spectrum (in  $d_8$ -THF) of the pale yellow powdery product shows a signal pattern similar to that observed for **2a,d** and **2c,b** (see Fig. S14 in ESI†). However, a prominent downfield shift of the signals is noticed: the singlet for the methylene hydrogens is observed at 5.09 ppm and the four aromatic multiplets are found between 7.58 and 9.17 ppm. A subsequent crystallographic analysis of the product showed it to be the neutral 1:1 adduct  $(\text{dpma})\text{InCl}_3$  (**3**) instead of an ionic compound. The crystal structure also contains a

molecule of the crystallization solvent that completes the octahedral coordination environment at the metal (Fig. 3). The neutral coordinated ligand in **3**·THF is bent in the same way to that in **1a**, **1b** and **2c**, with all other ligand related pertinent bond lengths and angles comparable between the four structures. The average In-N bond length in **3**·THF, 2.309(2) Å, is considerably shorter than that in a related complex  $\{[(dpma)InMe_2]^+[NO_3]^- \} \cdot H_2O$ , 2.431(4) Å, which is, however, ionic and significantly distorted from regular octahedral geometry.<sup>18b</sup> The packing of **3**·THF in the crystal lattice is similar to the salts **1a** and **1b** in that the adducts form layers along the crystallographic *c*-axis. The In-O distance in **3**·THF is 2.314(2) Å which is slightly shorter than that in a related THF adduct of an iminopyridine complex  $\{ArN=C(H)Py\}InCl_3 \cdot THF$ , 2.396(3) Å.<sup>22</sup>

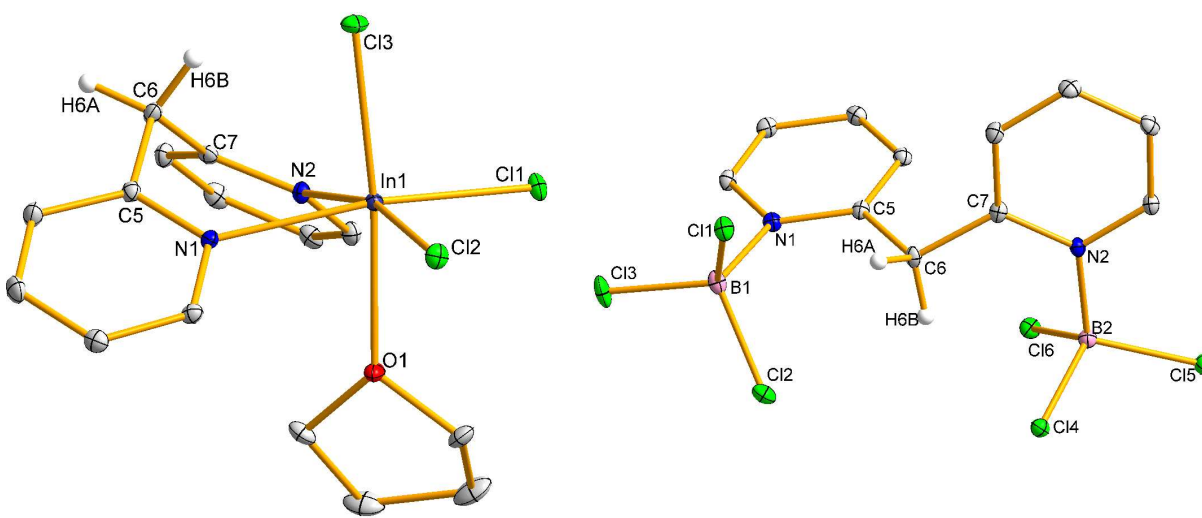


**Fig. 3** Thermal ellipsoid plots (30% probability) of the adducts (dpma)InCl<sub>3</sub>·THF (**3**·THF) (left) and (dpma)(BCl<sub>3</sub>)<sub>2</sub> (**4**) (right) as found in X-ray crystal structures. Hydrogen atoms on the pyridyl rings and the coordinated THF molecule have been omitted for clarity.

The reaction between dpma and InCl<sub>3</sub> in 1:2 stoichiometry in Et<sub>2</sub>O also gave a pale yellow and highly insoluble powder in low yield. Subsequent characterization of the product by <sup>1</sup>H NMR spectroscopy (in *d*<sub>8</sub>-THF) and X-ray crystallography showed the product to be the adduct **3** (see

Fig. S15 in ESI†). It is clear from these results that charge separation and subsequent formation of cations  $[(\text{dpma})_2\text{InCl}_2]^+$  and  $[(\text{dpma})\text{InCl}_2]^+$  are in this case energetically disfavoured processes.

**Reactions of dipyridylmethane (dpma) with  $\text{BCl}_3$  in 1:1 and 1:2 molar ratios.** A reaction between dpma and  $\text{BCl}_3$  was first performed using a 1:2 molar ratio of the reagents. The synthesis was carried out by the addition of  $\text{BCl}_3$  to  $\text{Et}_2\text{O}$  solution of dpma at  $-78\text{ }^\circ\text{C}$ , after which the reaction mixture was stirred for 1 h at room temperature. After removal of volatiles, the product was isolated as a fine off-white powder in good yield (86%). Single crystals of the product were obtained by slow diffusion from  $\text{CH}_2\text{Cl}_2$  and *n*-hexane.

The results from single crystal X-ray structural studies (Fig. 3) show that the 1:2 reaction between dpma and  $\text{BCl}_3$  gives a neutral diadduct  $(\text{dpma})(\text{BCl}_3)_2$  (**4**) instead of the salt  $[(\text{dpma})\text{BCl}_2]^+[\text{BCl}_4]^-$ . Clearly the formation of two Lewis acid-base interactions is in this instance energetically more favourable than charge separation and formation of a salt. Both B-N bond lengths in **4** (1.621(4) and 1.612(4) Å) fall within a typical range observed for related coordinate bonds (for example, 1.593(1) Å in a 1:1 complex between  $\text{BCl}_3$  and pyridine).<sup>23</sup> The structural flexibility of the dpma backbone ensures a sterically unhindered conformation for the adduct in which the pyridine rings adopt an almost perpendicular orientation, giving a structure that is close to  $C_2$  symmetry.

The  $^1\text{H}$  NMR spectrum of **4** (in  $\text{CD}_2\text{Cl}_2$ ) shows four multiplets for the pyridyl hydrogens from 7.43 to 9.82 ppm and a singlet for the bridge methylene hydrogens at 6.25 ppm which is shifted *ca.* 1.75 ppm downfield compared to the  $^1\text{H}$  NMR data of **2c** and **2d** (see Fig. S16 in ESI†). The significant downfield shift of the methylene hydrogens can be attributed to the short

intramolecular H...Cl contacts that are observed in the structure of **4**. All signals in the  $^1\text{H}$  NMR spectrum of **4** are slightly broadened, which in this instance is anticipated due to the nearly unhindered rotation of the pyridine rings around the bridging methylene group.

To complete the series, an equimolar reaction between dpma and  $\text{BCl}_3$  was carried out by addition of  $\text{BCl}_3$  to a stirred solution of dpma in  $\text{Et}_2\text{O}$  at  $-78\text{ }^\circ\text{C}$ . After stirring for 3 h, a red solution formed that was found to contain multiple products based on  $^1\text{H}$  NMR spectroscopy. The reaction was therefore repeated in toluene, which, again, gave a red solution but also a yellow-orange precipitate.  $^1\text{H}$  NMR spectrum of the isolated powder (in  $\text{CD}_2\text{Cl}_2$ ) showed it to be a single product giving a singlet at 5.06 ppm as well as four multiplets between 7.92 and 8.51 ppm. Subsequent recrystallization from a mixture of  $\text{CH}_2\text{Cl}_2$  and pentane gave X-ray quality single crystals that were not of the expected product,  $[(\text{dpma})\text{BCl}_2]^+[\text{Cl}]^-$ , but that of the dipyridinium salt  $[\text{H}_2(\text{dpma})]^{2+}[\text{BCl}_4]^-[\text{Cl}]^-$  (see ESI† for details).

A detailed  $^1\text{H}$  NMR analysis (in  $\text{CD}_2\text{Cl}_2$ ) of the red solution phase showed it to be a mixture of three major products:  $(\text{dpma})(\text{BCl}_3)_2$ , *i.e.* **4**,  $[(\text{dpma})\text{BCl}_2]^+[\text{Cl}]^-$  and  $(\text{dpme})\text{BCl}_2$  (see ESI† for details). This suggests that the 1:1 reaction of  $\text{BCl}_3$  with dpma initially gives both the diadduct **4** and the corresponding monoadduct which then undergoes ring closure to yield the salt  $[(\text{dpma})\text{BCl}_2]^+[\text{Cl}]^-$ . However, since some uncoordinated dpma ligand remains in solution, proton abstraction from the methylene bridge of the  $[(\text{dpma})\text{BCl}_2]^+$  cation can take place, giving  $(\text{dpme})\text{BCl}_2$  and  $[\text{H}(\text{dpma})]^+[\text{Cl}]^-$ . This kind of reactivity has been reported for coordination complexes of related ligands with a methylene bridge and a 1,3-diimine core.<sup>24</sup> These simple transformations would therefore lead directly to the product mixture observed spectroscopically.

In order to test the above hypothesis, the 1:1 reaction between dpma and  $\text{BCl}_3$  was repeated in the presence of an equimolar amount of trimethylamine. As a stronger base, trimethylamine

should protonate more easily and crystallize out from the reaction mixture as the salt  $[\text{Et}_3\text{NH}]^+[\text{Cl}]^-$ . Consequently, the reaction should in this instance yield a single complex of the deprotonated dpme ligand *i.e.*  $(\text{dpme})\text{BCl}_2$ . In good agreement with this prediction, the reaction gave a red solution and a light orange precipitate of which the latter was confirmed to be the known salt  $[\text{Et}_3\text{NH}]^+[\text{Cl}]^-$  by  $^1\text{H}$  NMR spectroscopy. The room temperature  $^1\text{H}$  NMR spectrum (in  $\text{CD}_2\text{Cl}_2$ ) recorded for the red solution showed a singlet at 5.48 ppm and four multiplets, two doublets and two triplets, between 6.59 and 8.22 ppm (see Fig. S18 in ESI†). The relative integration of the signals is 1:8, which confirms the presence of an anionic dpme ligand *i.e.* the neutral complex  $(\text{dpme})\text{BCl}_2$ ; the identity of the product was subsequently confirmed by single crystal X-ray crystallography.<sup>25</sup>

**Comparison between group 13 complexes of bpy and dpma.** Interestingly, there are only a handful of crystallographically characterized examples of coordination complexes of the parent bpy ligand with aluminium or gallium. For example, the 1:1 reaction between  $\text{GaCl}_3$  and bpy is known to give the ionic compound  $[(\text{bpy})_2\text{GaCl}_2]^+[\text{GaCl}_4]^-$ ,<sup>19,26</sup> analogous to **1b**, whereas the aluminium salt  $[(\text{bpy})_2\text{AlCl}_2]^+[\text{Cl}]^-$  comparable to **1a**, has been obtained from 1:2 reaction between  $\text{AlCl}_3$  and bpy.<sup>21</sup> There are no reported crystallographic data of salts containing ions of the type  $[(\text{bpy})\text{MCl}_2]^+$  ( $\text{M} = \text{Al}, \text{Ga}$ ) that would be analogous to the cations in compounds **2a–d**. However, it is known that the reactions of group 13 halides with bpy are complex and depend on the solvent and stoichiometry.<sup>21,27</sup> No VT NMR data of these reactions have been published, but it has been concluded that the exclusive crystallization of specific salts may simply be a result of precipitation of the least soluble cation,<sup>21</sup> which therefore leaves the predominant solution species unknown. The results reported herein show that the dpma ligand displays complex

solution behaviour with both  $\text{AlCl}_3$  and  $\text{GaCl}_3$ , suggesting that the same could also be true for the bpy ligand. However, in all instances where crystal structures were obtained in this work (salts **1a**, **1b** and **2c**), the composition of the determined structure was indeed consistent with the predominant species present in solution.

There are a number of coordination complexes of bpy with indium. Most relevant to the work reported herein are the solvated adducts of  $(\text{bpy})\text{InCl}_3$  similar to **3**·THF. For example,  $(\text{bpy})\text{InCl}_3\cdot\text{H}_2\text{O}$  has been prepared from  $\text{InCl}_3$  and bpy in aqueous conditions.<sup>28</sup> The adduct is octahedral at indium and the chlorides adopt a *facial* arrangement. Due to the planarity of the bpy ligand, the In-N bond lengths (*ca.* 2.28 Å) are shorter and the N-In-N bond angle ( $71.98(9)^\circ$ ) narrower in  $(\text{bpy})\text{InCl}_3\cdot\text{H}_2\text{O}$  than in **3**·THF (*ca.* 2.31 Å and  $79.25(7)^\circ$ ). A similar adduct with the composition  $(\text{bpy})\text{InCl}_3\cdot\text{EtOH}$  has also been reported.<sup>28</sup> In addition to neutral adducts of the type  $(\text{bpy})\text{InCl}_3$ , a salt  $[(\text{bpy})\text{InCl}_2]\text{Cl}$  containing a cation similar to that in **2c** has been structurally characterized.<sup>29</sup> Unfortunately the quality of the crystallographic data for  $[(\text{bpy})\text{InCl}_2]\text{Cl}$  precludes any further discussion of its structure.

There are no structurally characterized examples of neutral diadducts of the type  $(\text{bpy})(\text{MCl}_3)_2$  for any of the group 13 elements ( $\text{M} = \text{B}, \text{Al}, \text{Ga}, \text{In}$ ). The compound most closely related to **4** is  $(\text{bpy})\text{B}(\text{C}_6\text{F}_5)_3$  in which only one of the two nitrogen atoms is coordinated to tris(pentafluorophenyl)borane.<sup>30</sup> This monodentate coordination mode naturally results from the large steric bulk of the  $\text{C}_6\text{F}_5$  rings in  $\text{B}(\text{C}_6\text{F}_5)_3$ . Despite the vast difference in size between  $\text{BCl}_3$  and  $\text{B}(\text{C}_6\text{F}_5)_3$ , the B-N bond length in  $(\text{bpy})\text{B}(\text{C}_6\text{F}_5)_3$  is 1.649(5) Å and therefore very much comparable to that in **4**, 1.621(4) Å. A second coordination compound of bpy with boron that is related to the chemistry of the dpma ligand examined herein is  $[(\text{bpy})\text{BCl}_2]^+[\text{Cl}]^-$ . This salt contains the cation  $[(\text{bpy})\text{BCl}_2]^+$  that is structurally similar to that in **2c**.<sup>31</sup> The compound was

synthesized by 1:1 reaction between  $\text{BCl}_3$  and bpy in  $\text{CH}_2\text{Cl}_2$  *i.e.* in an analogous fashion to what in the case of the dpma ligand resulted in the formation of a mixture of products due to the facile deprotonation of the coordinated dpma ligand.

A very interesting feature in the chemistry of the  $[(\text{bpy})\text{BCl}_2]^+[\text{Cl}]^-$  salt is the possibility to reduce the cation to the corresponding neutral radical  $[(\text{bpy})\text{BCl}_2]^\bullet$ .<sup>31</sup> Spectroscopic, crystallographic and computational studies revealed that the unpaired electron in this complex is fully confined to the ligand framework, thereby yielding the paramagnetic anion  $(\text{bpy})^{\bullet-}$  that has also been structurally characterized in another group 13 complex,  $(\text{bpy})_3\text{Al}$ .<sup>32</sup> The bpy ligand can also exist as a diamagnetic dianion,  $(\text{bpy})^{2-}$ , which in the context of group 13 chemistry has been characterized in compounds such as  $(\text{bpy})\text{BCl}$  and  $[\text{Li}(\text{THF})_4]^+[(\text{bpy})_2\text{Al}]^-$ .<sup>33,34</sup> Even though there are significantly more cases of singly or doubly reduced bpy ligands coordinated to transition metal centres,<sup>35</sup> ligand non-innocence is also a prominent feature in main group chemistry of bpy and that of group 13 elements in particular.

Having therefore established the scope of coordination chemistry for the dpma ligand with group 13 elements, we turned our attention to investigate its possible non-innocent behaviour and the possibility to form paramagnetic group 13 complexes containing the anionic  $(\text{dpma})^{\bullet-}$  radical.

**Computational investigations of the cations  $[(\text{dpma})\text{MCl}_2]^+$  and  $[(\text{dpma})_2\text{MCl}_2]^+$  ( $\text{M} = \text{Al}, \text{Ga}$ ).** Before pursuing electrochemical and chemical attempts to reduce the cations  $[(\text{dpma})\text{MCl}_2]^+$  ( $\text{M} = \text{Al}, \text{Ga}$ ) to the corresponding neutral radicals, their electronic structures, as well as that of  $[(\text{dpma})_2\text{MCl}_2]^+$ , were examined using density functional theory (DFT).

The PBE1PBE/def-TZVP optimized structures of the cations  $[(\text{dpma})\text{MCl}_2]^+$  and  $[(\text{dpma})_2\text{MCl}_2]^+$  ( $\text{M} = \text{Al}, \text{Ga}$ ) are in very good agreement with the data from X-ray

crystallographic analyses of **1a**, **1b** and **2c** (see ESI† for details). This was expected as there are no significant cation-anion interactions present in the crystal structures of any of the characterized salts. The computed theoretical data was used to calculate Gibbs free energies for the reactions  $[(dpma)_2MCl_2]^+ \rightarrow [(dpma)MCl_2]^+ + dpma$  ( $M = Al, Ga$ ) which were found to be endergonic by 49 and 23  $\text{kJ mol}^{-1}$  for  $M = Al$  and  $Ga$ , respectively. Even though the model reactions do not take into account the effect of the counter ion or solvent, the predicted trend is comparable to experimental observations and suggest facile ligand detachment from  $[(dpma)_2GaCl_2]^+$ , as already observed in the VT NMR experiments.

The intrinsic strength of metal-ligand bonding in  $[(dpma)MCl_2]^+$  ( $M = Al, Ga$ ) was examined by calculating the instantaneous interaction energies with respect to the free dpma ligand and a cationic  $[MCl_2]^+$  fragment in the geometries they adopt in the complex. Again, only the trends in the calculated values should be considered meaningful as the reported energies do not correspond to proper bond dissociation. The results show that the instantaneous interaction energies are 356 and 323  $\text{kJ mol}^{-1}$  per Al-N and Ga-N bond, respectively. Similar values were also obtained for the M-N bonds in cations  $[(dpma)_2MCl_2]^+$  as well as in  $[(bpy)MCl_2]^+$  (340 and 307  $\text{kJ mol}^{-1}$  for Al-N and Ga-N, respectively, which shows that, to a first approximation, the metal-ligand bonding is independent of the ligand type.

Fig. 4 depicts the singly occupied molecular orbitals (SOMOs) of  $[(dpma)GaCl_2]^\bullet$  and  $[(dpma)_2GaCl_2]^\bullet$ ; the SOMOs of the corresponding aluminium cations are analogous and are not shown. In both cases the SOMO has virtually no contribution from the metal, indicating that the reductions are ligand centred. The SOMO of  $[(dpma)GaCl_2]^\bullet$  is comparable to the LUMO of the free dpma ligand, showing a delocalized  $\pi$ -system on both pyridyl rings and a node at the methylene bridge carbon due to the bent geometry of the ligand. In contrast, the SOMO of

$[(dpma)_2GaCl_2]^{\bullet}$ , while retaining much of the shape of the LUMO of free dpma, is delocalized to both of the ligands in the complex.

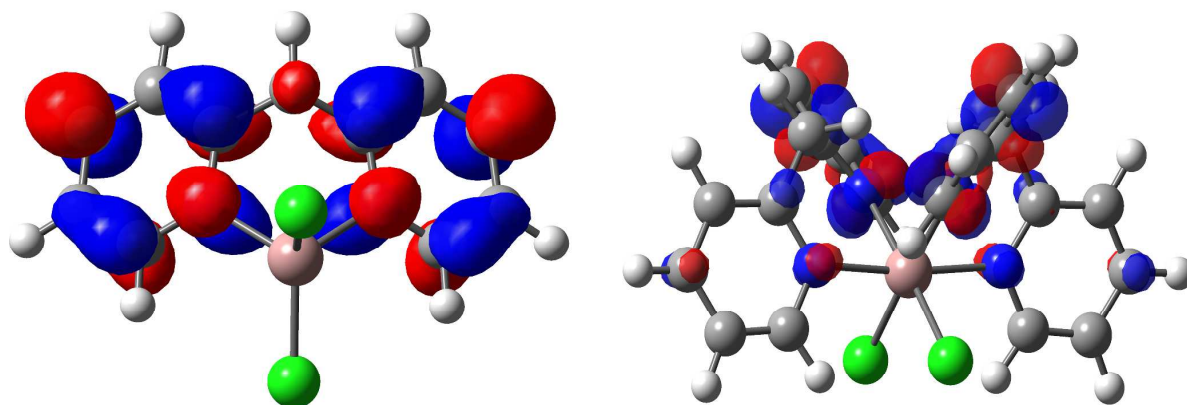


**Fig. 4** Isosurface plots of the SOMOs of the radicals  $[(dpma)GaCl_2]^{\bullet}$  (left) and  $[(dpma)_2GaCl_2]^{\bullet}$  (right).

The vertical electron affinities (VEAs) calculated for the cations  $[(dpma)MCl_2]^+$  and  $[(dpma)_2MCl_2]^+$  are both positive and virtually independent of the metal: *ca.* 4.5 and 3.7 eV for  $[(dpma)MCl_2]^+$  and  $[(dpma)_2MCl_2]^+$ , respectively. While all complexes are predicted to be reasonable electron acceptors, the calculated values are significantly lower than the VEA calculated for the cation  $[(bpy)BCl_2]^+$  (5.5 eV) that is known to give the neutral radical  $[(bpy)BCl_2]^{\bullet}$ .<sup>31</sup> The difference in the calculated VEAs for  $[(dpma)MCl_2]^+$  and  $[(bpy)BCl_2]^+$  can be understood in terms of the electronic structure of the ligand: the VEA for dpma is negative (–0.6 eV) while that of bpy is essentially zero (0.1 eV). Hence, the dpma ligand will not accept an electron unless it is coordinated to a metal centre. The energies of the LUMOs for the cations  $[(dpma)MCl_2]^+$  and  $[(dpma)_2MCl_2]^+$  follow the same trend as VEAs, which suggests that the former are more easily reduced than the latter. For these reasons, the electrochemical behaviour of the cations  $[(dpma)MCl_2]^+$  was put to the fore.

**Electrochemical and chemical reduction of  $[(dpma)MCl_2]^+[MCl_4]^-$  ( $M = Al, Ga$ ).** The electrochemical properties of the dpma ligand as well as that of the salts **2a–d** were investigated with cyclic voltammetry (CV) using a Pt electrode and  $[(n-Bu)_4N]^+[PF_6]^-$  as the supporting electrolyte. The free dpma ligand was found to be redox innocent within the potential window of the  $CH_3CN$  solvent (see Fig. S19 in ESI†) as expected based on its negative VEA. As shown by  $^1H$  NMR investigations, the aluminium salts **2b** and **2d** are stable in  $CD_3CN$ , but **2a** converts to the free dpma ligand, while **2c** contains a very small amount of **1a**. Consequently, the primary cationic species present in  $CH_3CN$  solutions of **2a–d** is  $[(dpma)MCl_2]^+$  ( $M = Al, Ga$ ). This is well corroborated by CV studies which showed a non-reversible reduction at nearly the same potential for **2a** and **2c** ( $M = Ga$ ;  $E_p^c = -0.95$  V; Fig. 5) and **2b** and **2d** ( $M = Al$ ,  $E_p^c = -1.11$  V; see Fig. S20 in ESI†), in agreement with the redox process  $[(dpma)MCl_2]^+ + e^- \rightarrow [(dpma)MCl_2]^{\bullet}$ . The difference in the cathodic peak potentials for the aluminium and gallium complexes is consistent with the role of the metal to tune the potential to a more accessible range than in the uncoordinated ligand, with the heavier metal having the stronger influence.<sup>36</sup>

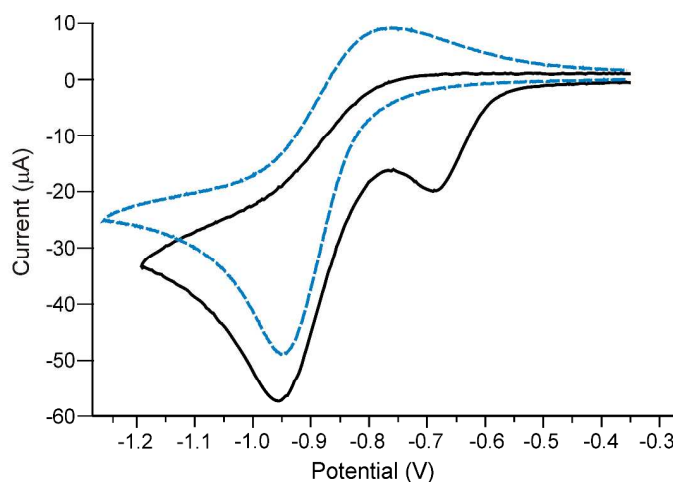


**Fig. 5** Cyclic voltammograms of **2a** (dashed line, 5.2 mM) and **2c** (solid line, 6.3 mM) in  $CH_3CN$  solutions containing 0.4 M  $[(n-Bu)_4N]^+[PF_6]^-$  at a Pt electrode at room temperature,  $v = 0.2$   $Vs^{-1}$ .

An interesting feature in the CV of **2c** is the preliminary wave at *ca.*  $-0.65$  V; a similar feature was not observed for **2a** or the aluminium systems **2b** and **2d**. We are unsure of the origin of this process, though it was observed that the preliminary wave is significantly smaller in  $\text{CH}_2\text{Cl}_2$  (see Fig. S21 in ESI†) and disappears entirely when the sample is titrated with extraneous  $[\text{Cl}]^-$  (see Fig. S22 in ESI†). It is tempting to assign the process to the reduction of the cation  $[(\text{dpma})_2\text{GaCl}_2]^+$  that is a minor species present in the  $\text{CH}_3\text{CN}$  solution of **2c**, but this assignment is not supported by the calculated VEAs that show  $[(\text{dpma})_2\text{GaCl}_2]^+$  to be reduced less readily than  $[(\text{dpma})\text{GaCl}_2]^+$ . One plausible scenario is, however, that the pre-reduction wave is a surface-confined process, resulting from strong adsorption of  $[(\text{dpma})\text{GaCl}_2]^\bullet$  on the electrode and eliminating chloride as this process would become evident only in solutions that are not saturated with  $[\text{Cl}]^-$  *i.e.* **2c**.

Despite the appearance of a preliminary wave in the CV of **2c**, the data for **2a–d** is consistent with a single ligand-centred redox process that is nearly identical to all systems investigated. Although the CVs of **2a**, **2b** and **2d** show a hint of a return wave, the stability of the radical species  $[(\text{dpma})\text{MCl}_2]^\bullet$  was insufficient to allow for detection of an EPR signal by *in situ* simultaneous electrochemistry and electron paramagnetic resonance spectroscopy. Indeed, several aspects point to significant instability of the reduction products: reduction potentials at glassy carbon electrode show characteristics of surface-confined processes with a strong cathodic shift, fouling of the electrode surface, total absence of reverse peaks and, most importantly, strong induction of chloride oxidation waves on the return scan. In this respect, if the reduction of  $[(\text{dpma})_2\text{MCl}_2]^+$  leads to the loss of chloride, the formed radicals  $[(\text{dpma})\text{MCl}]^{\bullet+}$  are metal, not ligand, centred and therefore extremely reactive. The instability of the reduction products,

whatever their identity, is also seen in chemical reduction experiments conducted using cobaltocene and sodium naphthalenide. Regardless of the colour changes observed during the reactions,  $^1\text{H}$  NMR spectroscopy showed the products to be complex mixtures and crystallization attempts yielded only diamagnetic side products such as the salt  $[\text{Cp}_2\text{Co}]^+[\text{GaCl}_4]^-$  or salts containing the pyridinium cation.

## Conclusions

In this comprehensive study, the reactions of dipyridylmethane (dpma) with  $\text{MCl}_3$  ( $\text{M} = \text{B}, \text{Al}, \text{Ga}, \text{In}$ ) were investigated in 1:1 and 1:2 stoichiometries with the primary interest in charting the coordination chemistry of the ligand and in the possibility to observe non-innocent ligand behaviour via one-electron reduction of the cations  $[(\text{dpma})\text{MCl}_2]^+$ .

The 1:1 and 1:2 reactions between dpma and  $\text{AlCl}_3$  in  $\text{CH}_3\text{CN}$  yielded the salts  $[(\text{dpma})\text{AlCl}_2]^+[\text{Cl}]^-$  (**2b**) and  $[(\text{dpma})\text{AlCl}_2]^+[\text{AlCl}_4]^-$  (**2d**), respectively. Mixtures of products were obtained if the same reactions were performed in  $\text{Et}_2\text{O}$ , allowing the spectroscopic and structural characterization of the salt  $[(\text{dpma})_2\text{AlCl}_2]^+[\text{AlCl}_4]^-$  (**1b**). The analogous reactions employing  $\text{GaCl}_3$  gave  $[(\text{dpma})_2\text{GaCl}_2]^+[\text{GaCl}_4]^-$  (**1a**) and  $[(\text{dpma})\text{GaCl}_2]^+[\text{Cl}]^-$  (**2a**) if performed in  $\text{Et}_2\text{O}$  and using an equimolar amount of reagents. With 1:2 stoichiometry, the reaction between dpma and  $\text{GaCl}_3$  yielded the salt  $[(\text{dpma})\text{GaCl}_2]^+[\text{GaCl}_4]^-$  (**2c**).

In contrast to the charge separated products obtained from the reactions of dpma with  $\text{AlCl}_3$  and  $\text{GaCl}_3$ , similar reactions with  $\text{BCl}_3$  and  $\text{InCl}_3$  in  $\text{Et}_2\text{O}$  led to the characterization of neutral adducts. In the case of  $\text{InCl}_3$ , the adduct  $(\text{dpma})\text{InCl}_3 \cdot \text{THF}$  (**3**·THF) was obtained as the sole product irrespective of the stoichiometry employed. Conversely, the outcome of the reaction employing  $\text{BCl}_3$  was dependent on the molar ratio of reagents. While 1:2 stoichiometry afforded

the diadduct  $(dpma)(BCl_3)_2$  (**4**), the use of an equimolar amount of reagents resulted in a mixture of products and subsequent deprotonation of the *dpma* ligand to give the neutral complex  $(dpme)BCl_2$ .

The results of this work can be compared to the chemistry of the ubiquitous bipyridine (*bpy*) ligand with group 13 trihalides. Computational data shows that the intrinsic metal-ligand bond strengths in the examined complexes are virtually independent of the ligand type. Thus, as far as the bond strength is concerned, the *dpma* ligand should have wide applicability in coordination chemistry. Furthermore, the presence of a methylene bridge in the *dpma* ligand renders the structural versatility of its complexes more varied than that observed for *bpy*. This is best exemplified by the notion that there are no crystallographically characterized examples of cations  $[(bpy)MCl_2]^+$  ( $M = Al, Ga$ ) or neutral adducts  $(bpy)(MCl_3)_2$  ( $M = B$ ). However, the methylene bridge in the *dpma* ligand is also a potential site for further reactivity and can be readily deprotonated by bases, as exemplified by the conversion of  $[(dpma)BCl_2]^+[Cl]^-$  to  $(dpme)BCl_2$ .

Despite the suitable coordinating properties of *dpma*, the results from electrochemical reduction experiments show it to be a poor electron acceptor. Coordination to a group 13 metal can be used to tune the reduction potential of the ligand to a more accessible range, but the purported radicals  $[(dpma)MCl_2]^\bullet$  ( $M = Al, Ga$ ) were found to be highly unstable, possibly dissociating chloride to yield metal centred radicals with fleeting existence. The different redox behaviour of *dpma* with respect to *bpy* can be rationalized with the electronic structure of the ligand and the presence of a methylene bridge in particular. This conclusion is further supported by our recent EPR spectroscopic characterization of the persistent spirocyclic radical  $[(dpme)_2Al]^\bullet$  in which the ligand is deprotonated and has a methene, not methylene, bridge.

With these features and characteristics of the dpma ligand in mind, we are currently continuing our investigations on redox non-innocent dpme and related nacnac-type ligands in main group complexes. Furthermore, we are also examining the possibility to take use of the facile reactivity observed for the methylene bridge in dpma to perform further ligand functionalization not possible for bpy. Preliminary results indicate that dpma is a useful and currently unexplored building block for new types of heteroscorpionate ligands. These represent one of the most versatile types of tridentate ligands that can coordinate to a wide variety of elements across the periodic table. The results of these investigations will be reported in due course.

### **Acknowledgements**

The authors gratefully acknowledge financial support from the Natural Sciences and Engineering Research Council of Canada, the Academy of Finland and the Technology Industries of Finland Centennial Foundation. Esa Haapaniemi and Elina Hautakangas are thanked for their assistance in NMR spectroscopy and elemental analyses, respectively. Veera Puhakka and Samu Forsblom are acknowledged for performing the preliminary reactions of the dpma ligand with  $\text{BCl}_3$ .

### **Notes and references**

<sup>a</sup> University of Jyväskylä, Department of Chemistry, Nanoscience Centre, P.O. Box 35, FI-40014 University of Jyväskylä, Finland. Phone: +358-40-805-3713, Fax: +358-14-260-2501, E-mail: [heikki.m.tuononen@jyu.fi](mailto:heikki.m.tuononen@jyu.fi)

<sup>b</sup> Department of Chemistry and Biochemistry, University of Lethbridge, Lethbridge, AB, Canada T1K 3M4.

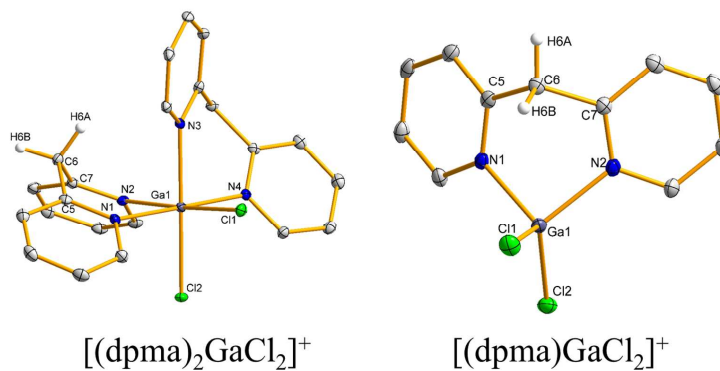
† Electronic Supporting Information (ESI) available: X-ray crystallographic files of **1a**·CH<sub>2</sub>Cl<sub>2</sub>, **1b**·THF, **2c**, **3**·THF and **4** in CIF format, crystallographic data and selected bond lengths and angles, <sup>1</sup>H NMR spectra and details of variable temperature NMR experiments, X-ray crystallographic characterization data of [H<sub>2</sub>(dpma)]<sup>2+</sup>[BCl<sub>4</sub>]<sup>-</sup>[Cl]<sup>-</sup>, additional CV data and DFT optimized structures of dpma, [(dpma)MCl<sub>2</sub>]<sup>+</sup>, [(dpma)<sub>2</sub>MCl<sub>2</sub>]<sup>+</sup> and [(dpma)MCl<sub>2</sub>]<sup>•</sup> (M = Al, Ga).

1. Cambridge Structural Database System 5.36: F. H. Allen, *Acta Crystallogr., Sect. B: Struct. Sci.*, 2002, **58**, 380–388.
2. (a) V. Balzani, F. Scandola, *Supramolecular Photochemistry*, Horwood: Chichester, U.K., 1991. (b) A. Juris, V. Balzani, F. Barigelletti, S. Campagna, P. Belser, A. von Zelewsky, *Coord. Chem. Rev.*, 1988, **84**, 85–277. (c) V. Balzani, A. Juris, M. Venturi, S. Campagna, S. Serroni, *Chem. Rev.*, 1996, **96**, 759–834. (d) E. A. Medlycott, G. S. Hanan, *Chem. Soc. Rev.*, 2005, **34**, 133–142. (e) E. A. Medlycott, G. S. Hanan, *Coord. Chem. Rev.*, 2006, **250**, 1763–1782.
3. (a) D. M. Klassen, G. A. Crosby, *J. Chem. Phys.*, 1965, **43**, 1498–1503. (b) G. A. Crosby, R. J. Watts, D. H. W. Carstens, *Science*, 1970, **170**, 1195–1196. (c) A. D. Gafney, A. W. Adamson, *J. Am. Chem. Soc.*, 1972, **94**, 8238–8239.
4. (a) X. Zhou, D. Zhu, Y. Liao, W. Liu, H. Liu, Z. Ma, D. Xing, *Nature Protocols*, 2014, **9**, 1146–1159. (b) H. Wei, E. Wang, *Luminescence*, 2011, **26**, 77–85.
5. (a) T. P. Yoon, M. A. Ischay, J. Du, *Nature Chem.*, 2010, **2**, 527–532. (b) D. A. Nicewicz, D. W. C. MacMillan, *Science*, 2008, **322**, 77–80.
6. F. Zhang, C. W. Kirby, D. W. Hairsine, M. C. Jennings, R. J. Puddephatt, *J. Am. Chem. Soc.*, 2005, **127**, 14196–14197.
7. A. Abo-Amer, M. S. McCready, F. Zhang, R. J. Puddephatt, *Can. J. Chem.*, 2012, **90**, 46–54.
8. (a) B. A. McKeown, H. E. Gonzalez, T. Michaelos, T. B. Gunnoe, T. R. Cundari, R. H. Crabtree, M. Sabat, *Organometallics*, 2013, **32**, 3903–3913. (b) B. A. McKeown, H. E. Gonzalez, T. B. Gunnoe, T. R. Cundari, M. Sabat, *ACS Catal.*, 2013, **3**, 1165–1171.
9. J. Moilanen, J. Borau-Garcia, R. Roesler, H. M. Tuononen, *Chem. Commun.*, 2012, **48**, 8949–8951.
10. A. B. Nepomnyashchii, A. J. Bard, *Acc. Chem. Res.*, 2012, **45**, 1844–1853.
11. A. Altomare, M. C. Burla, M. Camalli, G. L. Cascarano, C. Giacovazzo, A. Guagliardi, A. G. G. Moliterni, G. Polidori, R. Spagna, *J. Appl. Cryst.*, 1999, **32**, 115–119.

12. G. M. Sheldrick, *Acta Crystallogr., Sect. A: Found. Crystallogr.*, 2008, **64**, 112–122.
13. O. V. Dolomanov, L. J. Bourhis, R. J. Gildea, J. A. K. Howard, H. Puschmann, *J. Appl. Cryst.*, 2009, **42**, 339–341.
14. Gaussian 09, Revision D.01, M. J. Frisch, G. W. Trucks, H. B. Schlegel, G. E. Scuseria, M. A. Robb, J. R. Cheeseman, G. Scalmani, V. Barone, B. Mennucci, G. A. Petersson, H. Nakatsuji, M. Caricato, X. Li, H. P. Hratchian, A. F. Izmaylov, J. Bloino, G. Zheng, J. L. Sonnenberg, M. Hada, M. Ehara, K. Toyota, R. Fukuda, J. Hasegawa, M. Ishida, T. Nakajima, Y. Honda, O. Kitao, H. Nakai, T. Vreven, J. A. Montgomery, Jr., J. E. Peralta, F. Ogliaro, M. Bearpark, J. J. Heyd, E. Brothers, K. N. Kudin, V. N. Staroverov, R. Kobayashi, J. Normand, K. Raghavachari, A. Rendell, J. C. Burant, S. S. Iyengar, J. Tomasi, M. Cossi, N. Rega, J. M. Millam, M. Klene, J. E. Knox, J. B. Cross, V. Bakken, C. Adamo, J. Jaramillo, R. Gomperts, R. E. Stratmann, O. Yazyev, A. J. Austin, R. Cammi, C. Pomelli, J. W. Ochterski, R. L. Martin, K. Morokuma, V. G. Zakrzewski, G. A. Voth, P. Salvador, J. J. Dannenberg, S. Dapprich, A. D. Daniels, Ö. Farkas, J. B. Foresman, J. V. Ortiz, J. Cioslowski, and D. J. Fox, Gaussian, Inc., Wallingford CT, 2009.
15. (a) J. P. Perdew, K. Burke, M. Ernzerhof, *Phys. Rev. Lett.*, 1996, **77**, 3865–3868. (b) J. P. Perdew, K. Burke, M. Ernzerhof, *Phys. Rev. Lett.*, 1997, **78**, 1396. (c) J. P. Perdew, M. Ernzerhof, K. Burke, *J. Chem. Phys.*, 1996, **105**, 9982–9985. (d) C. Adamo, V. Barone, *J. Chem. Phys.*, 1999, **110**, 6158–6170.
16. A. Schäfer, C. Huber, R. Ahlrichs, *J. Chem. Phys.*, 1994, **100**, 5829–5835.
17. G. Dyker, O. Muth, *Eur. J. Org. Chem.*, 2004, **21**, 4319–4322.
18. (a) H. Gornitzka, D. Stalke, *Organometallics*, 1994, **13**, 4398–4405. (b) A. J. Canty, L. A. Titcombe, B. W. Skelton, A. H. White, *J. Chem. Soc., Dalton Trans.*, 1988, 35–45. (c) A. J. Canty, K. Mills, B. W. Skelton, A. H. White, *J. Chem. Soc., Dalton Trans.*, 1986, 939–945.
19. R. Restivo, G. J. Palenik, *J. Chem. Soc., Dalton Trans.*, 1972, 341–344.
20. Variable temperature  $^1\text{H}$  NMR experiments performed in  $\text{CD}_3\text{CN}$  for **2b** and **2d** showed no changes in their spectra within temperature range  $-30$  to  $+30$  °C.
21. P. L. Bellavance, E. R. Corey, J. Y. Corey, G. W. Hey, *Inorg. Chem.*, 1977, **16**, 462–467.
22. R. J. Baker, C. Jones, M. Klotha, D. P. Mills, *New J. Chem.*, 2004, **28**, 207–213.
23. K. Töpel, K. Hensen, M. Trömel, *Acta Crystallogr., Sect. B: Struct. Sci.*, 1981, **37**, 969–971.
24. (a) M. Goto, Y. Ishikawa, T. Ishihara, C. Nakatake, T. Higuchi, H. Kurosaki, V. L. Goedken, *J. Chem. Soc., Dalton Trans.*, 1998, 1213–1222. (b) M. Goto, Y. Ishikawa, T. Ishihara, C. Nakatake, T. Higuchi, H. Kurosaki, V. L. Goedken, *Chem. Commun.*, 1997, 539–540. (c) J.-M. Giraudon, D. Mandon, J. Sala-Pala, J. E. Guerchais, J.-M. Kerbaol, Y. Le Mest, P. L'Haridon, *Inorg. Chem.*, 1990, **29**, 707–713.
25. Unpublished results.
26. A. Sofetis, C. P. Raptopoulou, A. Terzis, T. F. Zafiropoulos, *Inorg. Chim. Acta*, 2006, **359**, 3389–3395.
27. (a) A. J. Carty, *Can. J. Chem.*, 1968, **46**, 3779–3784. (b) J. Y. Corey, R. Lamberg, *Inorg. Nucl. Chem. Lett.*, 1972, **8**, 275–280.
28. M. A. Malyarick, S. P. Petrosyants, A. B. Ilyuhin, *Polyhedron*, 1992, **11**, 1067–1073.
29. Y.-J. Song, P.-C. Zhao, P. Zhang, Z.-B. Han, *Z. Anorg. Allg. Chem.*, 2009, **635**, 1454–1457.

30. S. J. Geier, A. L. Gille, T. M. Gilbert, D. W. Stephan, *Inorg. Chem.*, 2009, **48**, 10466–10474.
31. S. M. Mansell, C. J. Adams, G. Bramham, M. F. Haddow, W. Kaim, N. C. Norman, J. E. McGrady, C. A. Russell, S. J. Udeen, *Chem. Commun.*, 2010, **46**, 5070–5072.
32. S. Herzog, K. Geisler, H. Präkel, *Angew. Chem., Int. Ed. Engl.*, 1963, **2**, 47–48.
33. S. M. Mansell, N. C. Norman, C. A. Russell, *Dalton Trans.*, 2010, **39**, 5084–5086.
34. G. B. Nikiforov, H. W. Roesky, M. Noltemeyer, H.-G. Schmidt, *Polyhedron*, 2004, **23**, 561–566.
35. C. C. Scarborough, K. Wieghardt, *Inorg. Chem.*, 2011, **50**, 9773–9793.
36. (a) E. J. Thompson, L. A. Berben, *Angew. Chem., Int. Ed.*, in press. doi: 10.1002/anie.201503935. (b) T. W. Myers, T. J. Sherbow, J. C. Gettinger, L. A. Berben, *Dalton Trans.*, in press. doi: 10.1039/c5dt01541c

## Graphical abstract for the table of contents



A comprehensive study of the coordination properties of the dipyridylmethane (dpma) ligand was performed. The preparation of metal complexes of the type  $[(dpma)_2MCl_2]^+$ ,  $[(dpma)MCl_2]^+$ , (M = Al, Ga),  $(dpma)InCl_3$  and  $(dpma)(BCl_3)_2$  is described along with their structures, solution chemistry and electrochemical properties.